END EFFECT IN SEGMENTAL CHANNEL

S. M. Barbarash, V. A. Golodnyak,
S. Yu. Reutskii, and I. M. Tolmach

UDC 621.313.333:538.4

Design of MHD devices with segmental channels necessarily involves study of the characteristics of a given machine in the end zone near the current-feeding electrodes and in the region of dropping intensity of the applied magnetic field. One such problem has already been solved [1]. For high-voltage MHD pumps, however, the formulation of the problem in that study [1] does not adequately describe the real processes in a machine. Specifically, it does not account for the finite resistance of connecting jumpers and does not include the insulating gaps which separate a current-feeding electrode from the segmental channel part.

In this study will be solved the problem of the end zone in a segmental channel with an isotropically conducting medium. The problem is solved in the two-dimensional formulation and in the inductionless approximation for a strip $|x| < \infty$, $0 \leqslant y \leqslant b$ where $v = \text{const}$ and $B = B(x)$, electrodes $0-a_1$, $0-a_4$, insulators $\infty < x < 0$, a_4-a_3, a_1-a_2, and a segmental part (Fig. 1). The channel segmentation is assumed to be ideal. It is necessary to solve the equation

$$\Delta\varphi=0$$

for the boundary conditions

Translated from Magnitnaya Gidrodinamika, No. 3, pp. 111-114, July-September, 1982. Original article submitted November 26, 1981.

 0024-998X/82/1803-0304$07.50

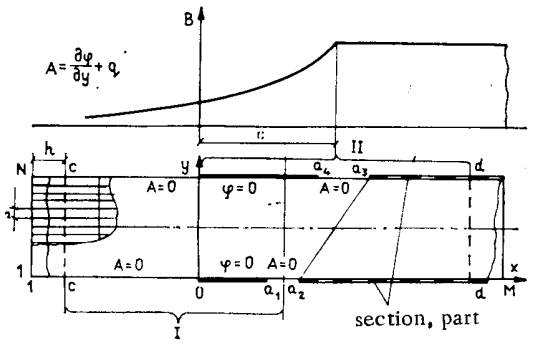

Fig. 1. Schematic diagram of electrode configuration in channel end zone.

$$\varphi=0,$$

at the electrodes,

$$\frac{\partial\varphi}{\partial y}+vB(x)=0,$$

and at the segmental part

$$\frac{\partial\varphi(x+\gamma b,b)}{\partial y}-\frac{\partial\varphi(x,0)}{\partial y}=vB(x)-vB(x+\gamma b),$$

$$\varphi(x+\gamma b,b)-\varphi(x,0)=-rb\left[\frac{\partial\varphi(x,0)}{\partial y}+vB(x)\right],$$

where r is the relative resistance of the connecting jumper.

After introduction of the dimensionless variables

$$\tilde{\varphi}=\frac{\varphi}{v_0B_0b},\quad \tilde{y}=\frac{y}{b},\quad \tilde{x}=\frac{x}{b},\quad q=\frac{vB}{v_0B_0},$$

with B_0 denoting the magnetic induction at infinity on the right-hand side, we assume that the magnetic induction drops from B_0 to zero in the end zone in any arbitrary manner.

The problem was solved with a rectangular grid

$$x=ih,\quad i=1\ldots M;$$

$$y=js,\quad j=1\ldots N,$$

where $h=\gamma\cdot s$.

The infinitely long strip was replaced with a rectangular one where the homogeneous solution for an ideal segmental channel was satisfied at the right-hand boundary d–d in the uniform-induction zone and where the condition of zero axial current component was satisfied at the boundary c–c, the locations of both boundaries to be determined as part of the solution of the problem. In order to facilitate the solution, the region under consideration was subdivided into two intersecting rectangles I and II so that one boundary of each had a known location and at those boundaries could be stipulated some boundary conditions such as, for instance, $\varphi = 0$. The location of the other boundary could then be determined during solution of the problem for each rectangle through stepwise shifting of that boundary until homogeneous conditions were satisfied within a region at some distance. After the locations of the boundary had been established, both solutions were collocated by the Schwartz method: the boundary conditions at the boundaries of the intersecting regions I and II were each time stipulated by values of the function found from the solution to the problem in the preceding

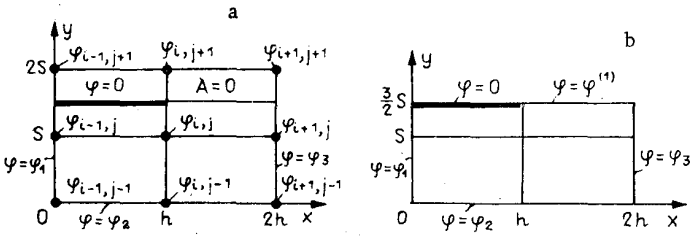

Fig. 2. Arrangement of grid nodes within the vicinity of contact between electrode and insulator (a) and region of problem solving for construction of difference scheme at point of discontinuity in boundary conditions (b).

iteration of the contiguous region. The problem was solved by the accelerated Liebman method [2] on a cruciform template, with the finite-difference approximation

$$\varphi_{i,j}^{(k+1)}=\frac{w}{2(1+\gamma^2)}\left[\gamma^2(\varphi_{i,j-1}+\varphi_{i,j+1})+\varphi_{i+1,j}+\varphi_{i-1,j}\right]+(1-w)\varphi_{i,j}^{(k)},$$

subscript k + 1 corresponding to the next approximation for $\varphi_{i,j}$ and w being the accelerating multiplier.

For approximating the boundary conditions $\varphi_{i,j}$ with a higher order of accuracy, the difference grid was shifted by a half-step [3] and the boundary conditions were written as

$$\varphi_{i,1}=-\varphi_{i,2},\quad \varphi_{i,N}=-\varphi_{i,N-1}$$

at the electrodes,

$$\varphi_{i,1}=\varphi_{i,2}+sq_i,\quad \varphi_{i,N}=\varphi_{i,N-1}-sq_i$$

at the insulators, and

$$\varphi_{i,1}=\frac{1}{r+s}\left[r\varphi_{i,2}+s\varphi_{i+N-2,N-2}-\frac{s^2}{2}q_{i+N-2}+\left(r+\frac{s}{2}\right)sq_i\right],$$

$$\varphi_{i,N}=\frac{1}{r+s}\left[r\varphi_{i,N-1}+s\varphi_{i-N+2}+\frac{s^2}{2}q_{i-N+2}-\left(r+\frac{s}{2}\right)sq_i\right]$$

at the segmental part.

As the initial approximation served the solution to the homogeneous problem, from which were also taken the initial boundary conditions for the corresponding boundaries of the rectangular regions I and II.

The iteration process for solving the problem was terminated as soon as the circuital law had been satisfied, within the given accuracy, at an electrode and inside the region. The locations of the boundaries of rectangles I and II were determined within a 5% accuracy.

At a point on the boundary between electrode and insulator there occurs a sharp change of potential, as such a point of discontinuity in the boundary conditions is approached. The potential at a grid node at such a discontinuity point and the current density distribution over an electrode were calculated by a difference scheme which had been constructed on the basis of the solution to the boundary-value problem for a rectangle taken around the adjacent grid nodes (Fig. 2a). The value of the potential at the boundaries was approximated with quadratic functions from known values at the grid nodes. The Laplace equation for the inside of a rectangle (Fig. 2b) was solved by the method of separation of variables, first for a rectangle $h\leqslant x\leqslant 2h$, $0\leqslant y\leqslant {}^3/_2 s$ and then for the entire region where the boundary condition $\partial\varphi/\partial y+q=0$ at an insulator had been replaced with the value of the potential found from the solution to the problem for that rectangle ($h\leqslant x\leqslant 2h$, $0\leqslant y\leqslant {}^3/_2 s$). The main characteristics can be expressed in a form derived from representation of a pump as a four-pole network [4], viz.

$$p_{ek}=K_{11}I+K_{12}Q,$$

$$V_k=K_{21}I+K_{22}Q,$$

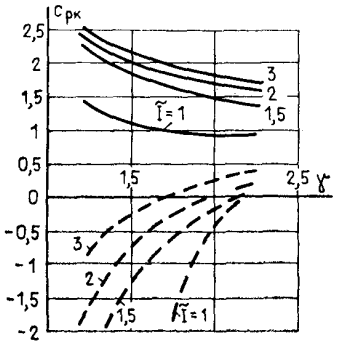

Fig. 3

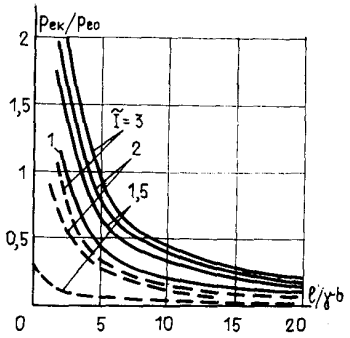

Fig. 4

Fig. 3. Dependence of the pressure head factor c_{pk} on the parameter of the connector parameter γ and on the operating mode $\tilde{I} = I_H/\sigma v B b^2$: solid lines correspond to lateral current feed, dash lines correspond to axial current feed.

Fig. 4. Relative pressure head developed in end zone, as function of relative channel length: solid lines correspond to lateral current feed, dash lines correspond to axial current feed.

with p_{ek} and V_k denoting, respectively, the pressure head and the voltage in the channel end zone between the boundaries c—c and d—d. The parameters of the end zone can then be described by only four coefficients $K_{i,j}$ depending on the geometry of the end zone, the relative resistance of the connector, the connector parameter γ, and the mode field intensity taper. It can be easily demonstrated that the correction to account for the electrically conducting shroud reduces to replacement of r with $(1+\xi)r$, where $\xi = 2\sigma_1\Delta_1/\sigma a$ is the shroud parameter.

Upon introduction of the ratio $c_{pk} = p_{ek}/p_{ek_o}$, where p_{ek_o} is the electromagnetic pressure head in a channel part as long as the segmental part of the end zone, one can compare the end zone with an equivalent to its channel part where the parameters are uniformly distributed, if the supply current and the flow rate are the same in both. The parameters of the end zone have been calculated for axial and lateral current feed nodes, the results are shown in Fig. 3.

Values of c_{pk} higher than unity signify that the end zone is equivalent, in terms of pressure head, to the channel part with uniformly distributed parameters and longer than the end zone, $c_{pk} < 1$ signifies the converse. It is also noteworthy that the operating mode of the channel plays an important role here and determines whether the end zone operates as a pump or as a brake ($c_{pk} < 0$). We deal here essentially with simultaneous operation of MHD channels connected in series (channel with segmental electrodes and end zones), the operations of which must be matched.

It is obvious that the role of the end zone in the operation of the machine becomes less significant as the length of the pump channel is increased. Upon referring the pressure head in the end zone to the total pressure head in the channel, one can easily determine at what relative length $\ell/\gamma b$ it is permissible to disregard the end zones. The graph in Fig. 4 indicates that for $\ell/\gamma b \geqslant 20$ the relative pressure head p_{ek}/p_{e_o} in one end zone is lower than 10%.

The results of experiments with model SN-5 MHD pumps under high voltage (two samples, one with 1 mm thick shroud and one with 2 mm thick shroud) were compared with calculations taking into account the channel end zones. The graph in Fig. 5 depicts the p—Q characteristics of these pumps, processed in the form [5]

$$\frac{p_a}{IB} = a_1 + b_1\frac{QB}{I} + c_1\frac{Q^2}{IB}, \text{ where } \frac{QB}{I} = \left(\frac{QB}{I}\right)_{exp} + \frac{c_1}{b_1}\left(\frac{Q^2}{IB}\right)_{exp}.$$

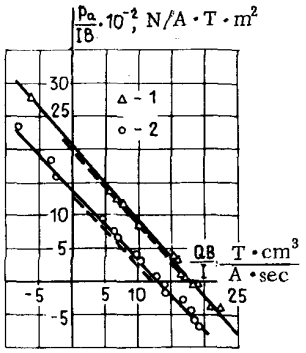

Fig. 5. Comparison of experimental data with calculations taking into account the end zone: 1) model SN-5-1 pump; 2) model SN-5-2 pump. Dash lines represent calculations.

The dash lines in Fig. 5 represent the theoretical characteristics, which do not differ from experimental ones by more than 10%, and this closeness correlates satisfactorily with the accuracy of the experimental setup (about 11%).

In this way, through solution of the problem, we have determined the contribution of the end zone to the total pressure head in a pump: an end zone of a relative length $l/\gamma b > 20$ need not be taken into account in the pump design. The calculations for a high-voltage MHD pump with the end zone taken into account agree closely with experimental data.

The solution to the problem and the results can be used for calculating the end effect in devices with a segmental channel.

LITERATURE CITED

1. G. P. Bazarov, É. N. Kufa, and S. A. Medin, "Commutation of electrodes at end zone of MHD series generator," Teplofiz. Vys. Temp., 15, No. 6, 1276-1283 (1977).
2. D. D. McCracken and W. S. Dorn, Numerical Methods with FORTRAN 4 Case Studies, Wiley (1972).
3. M. K. Gavurin, Lectures on Computation Methods [in Russian], Nauka, Moscow (1971).
4. Yu. A. Birzvalk, "Application of converter theory to electromagnetic conduction pump," Elektrichestvo, No. 6, 21-23 (1965).
5. Yu. A. Birzvalk, M. É. Broka, V. V. Duganov, D. S. Kovner, I. N. Mikryukova, A. V. Tananev, and Yu. P. Chernyaev, "Experimental study and general characteristics of channels of separately excited conduction pumps," Magn. Gidrodin., No. 4, 117-122 (1971).